ACS APPLIED MATERIALS & INTERFACES

Research Article

www.acsami.org

Aqueous Dispersions of Exfoliated Molybdenum Disulfide for Use in Visible-Light Photocatalysis

Matthew D. J. Quinn, Ngoc Han Ho, and Shannon M. Notley*

Faculty of Life and Social Sciences, Swinburne University of Technology, Hawthorn, 3122 Victoria, Australia

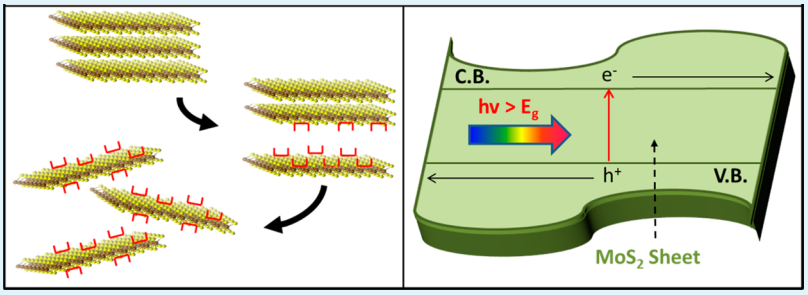

ABSTRACT: Single and few layer molybdenum disulfide (MoS_2) was exfoliated from the bulk form through a liquid phase exfoliation procedure. Highly concentrated suspensions were prepared that were stabilized against reaggregation through adsorption of nonionic polymers to the sheet surface. These exfoliated particles showed strong photoluminescence at an energy of 1.97 eV which is in the visible-light region. These exfoliated MoS_2 sheets were then used to catalyze the degradation of a model dye upon exposure to visible light.

KEYWORDS: *MoS_2, photocatalysis, photoluminescence, tunable band gap, two-dimensional particle, exfoliation*

INTRODUCTION

Atomic crystalline materials have received enormous recent interest, the most prominent example being graphene.[1,2] While graphene has rightly captured the attention of many researchers in diverse disciplines due to unique structural, thermal, mechanical, and electronic properties,[3−5] it is but one of a class of two-dimensional materials which include semiconductors such as the transition metal dichalcogenides WS_2 and MoS_2.[6−8] Like graphene, WS_2 and MoS_2 have vastly different properties in the limit of 2D in comparison with the bulk material. In particular, the optical and electronic properties vary significantly, with an increase in bandgap arguably the most important.

Recent studies by Splendiani et al.[9] and Mak et al.[10] have shown that MoS_2, an indirect semiconducting bulk material with a bandgap of 1.22 eV, is a direct bandgap (1.97 eV) semiconductor upon processing to a single layer.[9,10] Furthermore, strong photoluminescence is observed at 1.97 eV but only for single-layer MoS_2 with decreasing intensity for two and few layered material. Similarly, the analogous material WS_2 also demonstrates this transition from indirect to direct transition upon exfoliation.[11] Thus, exfoliation of MoS_2 represents a potential large-scale route for the production of a semiconducting material with a tunable bandgap which is capable of absorbing photons in the visible region. These single-layered transition metal dichalcogenides are hence of great interest in photocatalytic applications and, specifically, the splitting of water to produce hydrogen.

Bandgap properties of MoS_2 have been tuned in the past through quantum confinement of crystallites in 3D.[12,13] Typically the particle size dependent bandgap can be as high as 2.5 eV for nanoparticles in the range of 4−5 nm. However, 2D confinement through exfoliation to single sheets is also possible. Both experimental and theoretical studies have shown too that the position of the conduction band of single-layer MoS_2 is appropriate for the redox splitting of water. To produce hydrogen on an industrial scale, colloidal bed reactors are currently being investigated. One of the most important aspects though for this technology is the large-scale synthesis of appropriate semiconducting materials which are not only stable in water but also able to catalyze the reaction using the maximum amount of available solar radiation with high efficiency.

Aside from the potential use in hydrogen generation, there is also the possibility of using such materials in other catalytic applications. The positioning of the bands of single-layer MoS_2 is such that hydroxyl radicals may be formed which are capable of reacting with undesirable organic species in an aqueous environment. The ultrahigh surface area of exfoliated MoS_2 provides an added incentive for exploitation in this application as adsorption to the solid−liquid interface is essential.

There is hence a great interest in preparing stable aqueous suspensions of MoS_2 and other such materials. Most of the fundamental studies on the properties of the single and few layer MoS_2 have been performed on material produced using mechanical exfoliation or the so-called "Scotch Tape

Received: September 23, 2013
Accepted: November 25, 2013
Published: November 25, 2013

Method".[9,10] The adhesive tape procedure is clearly not a scalable process, so other techniques for producing exfoliated MoS_2 have been presented. One such method which has been extensively used in the production of graphene from graphite is surfactant-assisted sonication pioneered by the group of Coleman.[8,14−16] This is aqueous solution processing and hence has significant economic and environmental advantages over the use of organic solvents[17−19] or ionic liquids.[20,21] Chemical exfoliation through intercalation and subsequent exfoliation has also been used with similar issues of high cost and potential of degradation.[22]

In the surfactant-assisted sonication exfoliation technique, a suspension of particles is typically first prepared in an aqueous surfactant solution.[23−25] The type of surfactant is not overly important as long as it is capable of reducing the surface tension of the aqueous phase to match the cohesive energy of the van der Waals bonded solid.[4] Furthermore, the surfactant adsorbs to the exfoliated surfaces which aids in improving stability of the suspension against reaggregation. Hence, polymeric surfactants which are irreversibly adsorbed are highly suited to this application.[26,27] It should be recognized though that surfactant adsorption to the solid−liquid interface causes the surface tension of the aqueous phase to increase. This limits the extent of exfoliation. It has been recently shown that the concentration of exfoliated graphene particles can be increased if the surfactant is added continuously.[25] In this way, a constant stream of surfactant allows the maintenance of the surface tension to the optimum range of approximately 40−42 mJ/m^2, hence promoting continued exfoliation. Here, in this study, we present a scalable method for the production of large quantities of exfoliated MoS_2 nanoparticles suitable for use in photocatalytic applications.

EXPERIMENTAL SECTION

Materials. Powdered molybdenum(IV) sulfide (MoS_2), with a bulk particle size of <2 μm, was purchased from Sigma Aldrich and used as received. A typical method of preparing a MoS_2 sheet suspension is the surfactant-assisted liquid exfoliation technique. This technique relies on the surface energy of the material being approximately matched to the interfacial energy of the liquid medium. In this method, the addition of surfactant aids in lowering the interfacial energy of the liquid, while additionally preventing reaggregation upon exfoliation. Two different triblock copolymers were used in this study, P123 (poly(ethylene glycol)-block-poly(propylene glycol)-block-poly(ethylene glycol)), with a feed ratio of 20:70:20 (EO:PO:EO) and an average $M_n \sim 5.8$ kDa, and F127 with molecular weight of ∼12.5 kDa and nominal formula $(HO(CH_2CH_2O)_{101}(CH_2CH(CH_3)O)_{56}((CH_2CH_2O)_{101}H))$. All were purchased from Sigma Aldrich Australia and used without further purification. All suspensions were prepared using Milli Q water.

Methylene blue was also obtained from Sigma Aldrich and used in the photocatalysis experiments. Solutions were prepared in Milli-Q water. Prior to the introduction of the MoS_2 suspension, the pH of the methylene blue solution with a concentration of 25 mg/L was adjusted to 6.5 using an appropriate amount of HCl or NaOH.

Preparation of Exfoliated MoS_2 Suspension. Typically a 1% w/w suspension of bulk MoS_2 in Milli-Q filtered water is prepared in a 10 L reaction reservoir. The liquid solution was drawn through the Q700 Qsonica ultrasonicator, probe model CL-334, using a pump system, which cycles with the reaction reservoir. Ultrasonication was carried out continuously over the exfoliation period at ∼100 W.

A 10% w/w solution of the P123 surfactant and Milli-Q filtered water was added at a rate of 1 mL/min into the reaction reservoir over the course of the exfoliation time of 17 h. Regular 10 mL extractions were taken of the exfoliating MoS_2 solution to allow for characterization of samples representing different periods within the exfoliation process. The concentration of MoS_2 in suspension was determined from atomic absorption spectroscopy (AAS) (SpectrAA 200, Varian). The suspension was dissolved in a 1:1 solution of concentrated HNO_3 and HCl prior to measurement of the concentration of Mo, with the subsequent concentration of MoS_2 determined through consideration of the molecular stoichiometry.

To demonstrate the increase in concentration of the exfoliated MoS_2 over the course of the sonication period, the absorbance of each of the 10 mL extractions was measured using UV−visible spectrophotometry. The samples were centrifuged using the Rotofix 32 (Hettich) to remove the larger, unexfoliated particles to allow for an accurate representation of the concentration of exfoliated MoS_2. Centrifugation was carried out at 1500 rpm for 5 min, and the supernatant was extracted, avoiding the larger particles at the base of the centrifuge tube. Each sample was then placed in a Unisonics sonication bath for 5 min prior to UV−visible analysis. From the known concentration of MoS_2 determined using AAS and the absorbance at 800 nm from UV−vis spectrophotometry, the extinction coefficient of liquid phase exfoliated MoS_2 was determined to be 33.5 $L\ g^{-1}\ cm^{-1}$. This is higher than reported in a recent study of 29.2 $g\ L^{-1}\ cm^{-1}$ for chemically exfoliated MoS_2 prepared using the intercalation method.[22] This is reasonable as the MoS_2 sheets prepared through liquid phase exfoliation have fewer defects than the chemically exfoliated particles as demonstrated by measurements of surface potential (or electrophoretic mobility in this case).

Characterization of MoS_2 Particles. The MoS_2 particles dried from suspension were characterized by atomic force microscopy (AFM) to confirm that the sonication procedure produced single and few layered material. A Multimode 8 AFM from Bruker was used for imaging of the particles. Standard noncontact rectangular cantilevers with a nominal tip radius of 5 nm were used for the tapping mode imaging. The particles were dried onto a piece of oxidized silicon wafer and calcined at 450 °C to remove surfactant prior to measurement of the thickness and lateral size dimensions of the MoS_2 sheets.

The mean particle lateral size was also determined using a dynamic light scattering (DLS) technique developed by Lotya and the Coleman group who showed that the equivalent sphere radius scales with the particle size of a thin planar exfoliated sheet using eq 1[28] where a is the peak in the particle size distribution in nanometers. According to eq 1, a significant error in the determination of the particle size using this method may be expected. This is not surprising given that the particle size is determined from the autocorrelation function generated from diffusing particles. A 90Plus Particle Size Analyzer (Brookhaven Instruments) was used to measure equivalent sphere radius of the MoS_2 particulate suspension. This in turn was then used to calculate the mean lateral particle size. While there may be some error in the determination of nanosheet particles using this method, DLS does provide a useful first estimate and demonstrates that the particle size is significantly reduced upon exfoliation. The mean lateral particle size was hence determined from the peak of the particle size distribution and calculated to be 55 ± 5 nm.

$$L = (0.07 \pm 0.03)a^{1.5\pm0.15} \quad (1)$$

The exfoliated MoS_2 particles were characterized using Raman spectroscopy using an alpha 300A Raman system from WITEC with laser excitation at 532 nm. The particles were initially dried onto a silicon wafer prior to measurement. The photoluminescence spectrum of the exfoliated MoS_2 particles was also measured using the same laser excitation wavelength.

The exfoliated particles and bulk material were also characterized using UV−vis spectrophotometry which was carried out on the Cary 300 Bio UV−visible spectrophotometer (Varian). Samples were appropriately diluted in Milli-Q filtered water to ensure accurate absorbance readings. The spectra were recorded using quartz cuvettes in the wavelength range of 250−800 nm.

The zeta potential of the exfoliated MoS_2 nanoparticles was determined by a 90Plus Particle Size Analyzer from Brookhaven Instruments Corporation. The measurements were performed in Milli-Q water (pH 6.5). Typically five measurements of zeta potential using

four separate samples were undertaken. The value reported here is an average of these 20 measurements.

Photocatalytic Degradation of Methylene Blue Using Exfoliated MoS_2. The photodegradation of methylene blue in the presence of exfoliated MoS_2 was investigated upon exposure to a white light source. In a typical experiment, a solution of methylene blue was added to a suspension of MoS_2 (20 ppm as determined from spectrophotometry) in polypropylene and subjected to visible light from a xenon lamp with a 400 nm high pass filter. This low concentration of particles was used to demonstrate the efficiency of the catalyst. Furthermore, highly concentrated suspensions gave rise to significant scattering resulting in nonlinear effects in terms of light absorption as a function of concentration. After a given time, the MoS_2 particles were removed by centrifugation, and the relative concentration decrease of methylene blue was measured using spectrophotometry at a wavelength of 670 nm. Some samples were not exposed to light prior to centrifugation, allowing the concentration drop due to the adsorption onto the particles to be determined. Thus, the initial concentration of methylene blue, A_0, is reported as the concentration after adsorption yet prior to exposure to light. An additional experiment where the photocatalytic ability of bulk MoS_2 was used in place of the exfoliated nanosheets was also performed, although it is noted that mismatched bands are unlikely to result in the formation of reactive oxygen species. Rapid sedimentation of the particles however negated the possibility of further investigation.

RESULTS AND DISCUSSION

To prepare the single and few layer sheets of MoS_2, a liquid phase exfoliation procedure was undertaken in water with continuous surfactant addition. Previously, this method has been applied to the production of graphene with a significant increase in the overall concentration of particles produced. The surfactants used here in this study were block copolymer PEO−PPO−PEO type which allow the reduction and maintenance of the surface tension of the aqueous phase to the optimum level for efficient exfoliation as well as improving the stability of the suspended particles through adsorption onto the basal planes. Figure 1 shows the UV−visible spectra of exfoliated

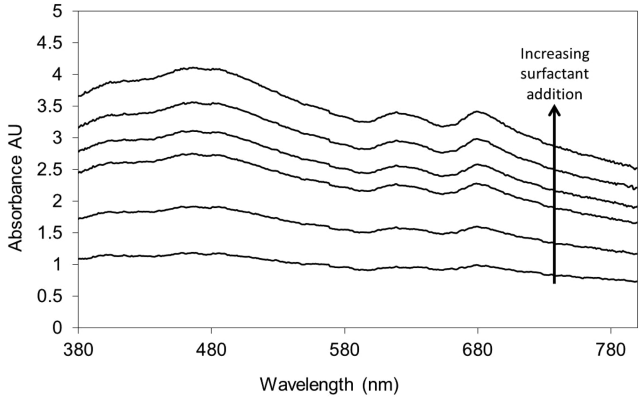

Figure 1. UV−visible spectra of exfoliated MoS_2 particles as a function of increasing addition of the surfactant P123 at a rate of 1 mL/min. Time series of curves from the bottom are 270, 360, 660, 750, 870, and 990 min.

suspensions of MoS_2 with increasing surfactant addition. The spectra are typical of MoS_2 suspensions, with no significant shift of the excitonic peaks due to confinement of the particles to single and few layers thicknesses. This is consistent with previous studies where a shift of the adsorption edge is only observed with confinement in three dimensions to length scales on the order of nanometers.

In Figure 1, the A and B excitonic peaks are easily distinguishable at 670 and 627 nm, respectively. These peaks are related to the direct excitonic transitions at the K point of the Brillouin zone with the energy difference arising due to spin−orbital splitting of the valence band. The absorption can be clearly seen to increase upon the continual, slow addition of the surfactant during sonication. Furthermore, with the lengthy sonication procedure at relatively high power, the observed UV−visible spectra are not altered, providing some evidence that there is a not a significant structural change to the exfoliated material through, for instance, bond scission.

Figure 2 shows the concentration of MoS_2 particles in suspension derived from the absorption at 800 nm as a function

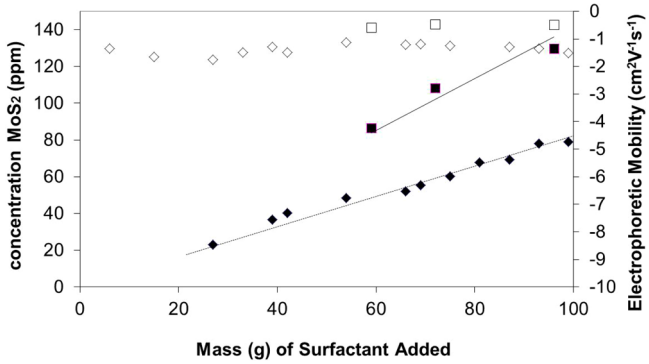

Figure 2. Concentration of MoS_2 in suspension determined from adsorption at 800 nm (using an extinction coefficient of 32 L g^{-1} cm^{-1}) and electrophoretic mobility of MoS_2 sheets as a function of surfactant addition for the two nonionic block-copolymer surfactants P123 (diamonds) and F127 (squares). Open symbols designate the electrophoretic mobility.

of the amount of surfactant added for both polymeric surfactants investigated in this study. There is a strong linear correlation between the amount of surfactant and the overall concentration of exfoliated MoS_2 particles for both surfactants. However the slopes are different which reflects the change in surface tension of the aqueous phase as a function of the concentration of surfactant (i.e., $d\gamma/dc$). The results in Figure 2 show that the use of the more hydrophilic block copolymer surfactant F127 results in a greater concentration of exfoliated MoS_2 particles. Also shown in Figure 2 is the measured electrophoretic mobility of the particles, again as a function of the surfactant added (which also relates to the length of time of sonication). There is no significant change in particle charge even with extended periods of sonication indicating little to no oxidation due to bond cleavage or cavitation. The electrophoretic mobility of the exfoliated MoS_2 sheets overall is low. While it is not completely appropriate to convert this to zeta potential due to the obviously irregular particle shape, to a first approximation the zeta potential would be of the order of −13 mV at pH 6.5. This would not normally give rise to a stable suspension, hence the use of the polymeric surfactants. These exfoliated MoS_2 particles are sterically stabilized. The extent of the polymer chains away from the interface is sufficient to prevent the close approach required for the attractive dispersion forces to dominate the overall interaction potential. Thus, these highly concentrated aqueous MoS_2 suspensions are stable over periods in excess of 6 months. The relatively high density though results in some sedimentation, although these particles are readily redispersed through simple agitation.

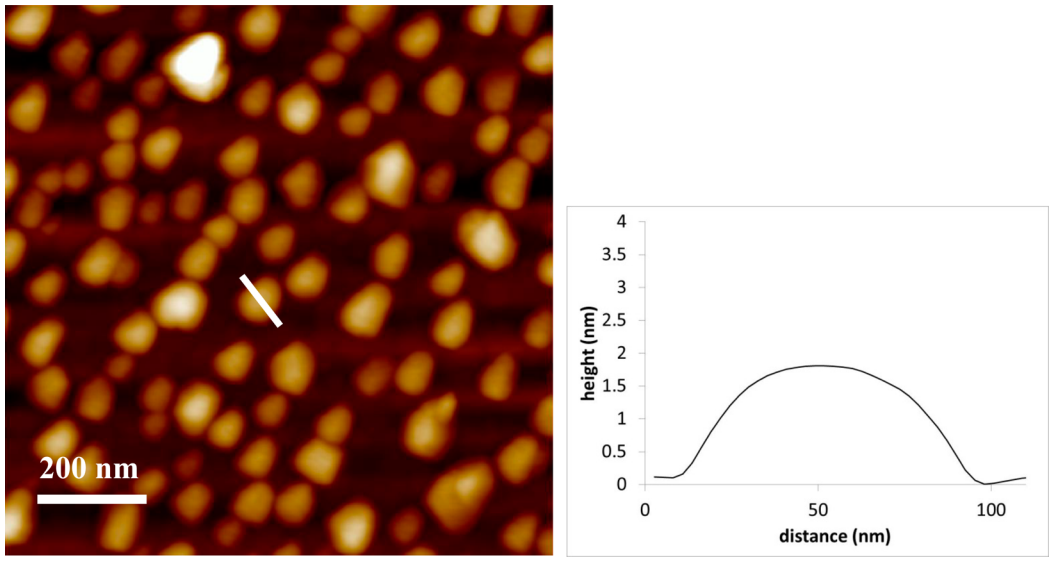

Figure 3. Left: Noncontact mode AFM images of exfoliated MoS_2 particles. Scan size is 1 μm × 1 μm. Particles range in lateral dimension from 50 to 90 nm. Right: Cross section over particle marked in the image showing height variation. (Particle appears rounded due to AFM tip convolution.)

Individual MoS_2 particles were imaged using atomic force microscopy in noncontact mode. In a typical experiment, the suspension was dried on silicon wafer. Figure 3 shows representative images of the exfoliated particles. The MoS_2 sheets have lateral dimensions of the order of 50−90 nm with irregular shape which is consistent with the measurement of mean lateral particle size determined from dynamic light scattering of 55 nm. As can be seen from the images in Figure 3, the exfoliation procedure produces polydisperse particles in terms of not only the lateral dimensions but also thickness. The majority of particles though has a thickness of 1.5−2 nm which suggests that the exfoliated MoS_2 sheets are predominantly single layer.

The exfoliated MoS_2 particles were also characterized using Raman spectroscopy. This experimental technique has proven to be highly useful in demonstrating changes in electronic properties of van der Waals bonded materials as the thickness approaches a single layer. Peak position and intensity have been used to demonstrate the number of layers of material as well as the presence of any defects. The MoS_2 suspension prepared through the surfactant-assisted sonication technique was deposited onto the silicon wafer prior to measurement. Figure 4 shows the spectrum for the bulk material as well as the exfoliated particles in the region of 360−420 cm^{-1}. Two peaks are observed in the bulk MoS_2 at 380 and 408 cm^{-1} which are designated as the E_{2g} and A_{1g} peaks, respectively. The A_{1g} peak is the out-of-plane phonon mode, which is predominantly related to the stretching of the sulfur atoms. The E_{2g} peak is the in-plane bending mode. Upon exfoliation of the bulk material to single and few layered MoS_2, the E_{2g} peak blue shifts to 382 cm^{-1}, and the A_{1g} red shifts to 406 cm^{-1}. The peak shifts observed here are in agreement with the ab initio calculations of Molina−Sanchez and Wirtz, in terms of magnitude for single layer MoS_2 sheets.[29]

Previous experimental studies have shown a greater red shift in the position of the A_{1g} peak for single particle measurements, where the difference between peak positions ($\Delta\omega = A_{1g} - E_{2g}$) can be decreased by as much as 6 cm^{-1}. The observed $\Delta\omega$ as shown in Figure 4 is ∼4 cm^{-1} which is greater in magnitude than previously observed for a bilayer sheet suggesting that the

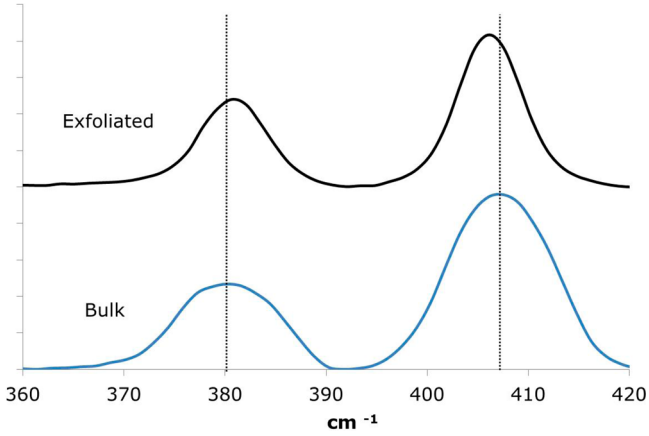

Figure 4. Raman spectra of bulk MoS_2 (lower) and exfoliated MoS_2 particles (upper) deposited onto a silicon wafer.

exfoliated particles measured here are likely to be only a single layer thick. The decrease in frequency of the A_{1g} peak arises from the reduction in the weak interlayer attractive forces between sulfur atoms in adjacent planar sheets upon exfoliation to a single layer. However, the observed increase in frequency of the E_{2g} peak, which is related to the in-plane bending mode, cannot be rationalized in the same way. It has been suggested though that the increase in frequency is due to the Coulombic interactions which are much longer in range, observations which have been supported by calculation. Interestingly, no significant change in the relative intensities of the peaks was observed; however, the width of the peaks for the exfoliated particles is less than the bulk MoS_2.

The emerging photoluminescence phenomenon of MoS_2 prepared using mechanical exfoliation has previously been investigated.[9,10] Similarly, the analogous material WS_2 was also shown to photoluminesce in the limit of 2D or toward a thickness of a single layer, when prepared using a liquid phase exfoliation technique.[11] The photoluminescence spectrum of the exfoliated MoS_2 particles produced here was measured under laser excitation at 532 nm. Figure 5 shows that the MoS_2 sheets exhibit a strong emission at 1.97 eV in agreement with

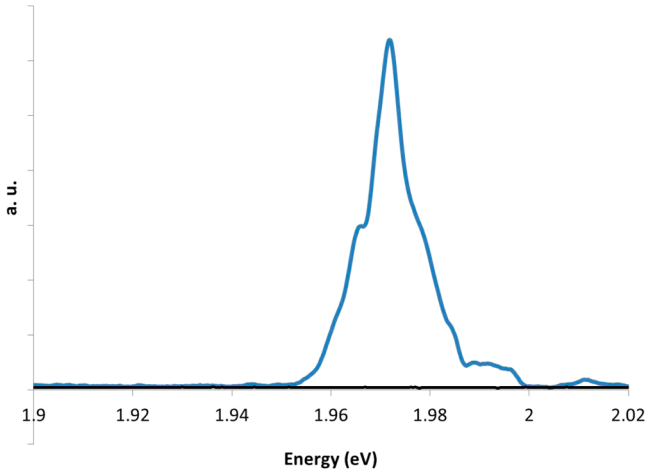

Figure 5. Photoluminescence spectrum of exfoliated MoS_2 particles (blue) dried on a silicon wafer using a laser with incident wavelength of 532 nm (2.33 eV). The PL spectrum of the underlying wafer is shown in black.

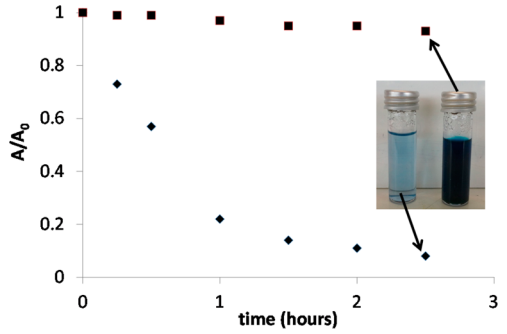

Figure 6. Photodegradation of methylene blue as a function of time in the presence of 20 ppm of exfoliated MoS_2 particulate suspension. Light with a wavelength of greater than 400 nm was used. The sample exposed to light (diamonds) showed a rapid decrease in the intensity of the light absorbed with time, whereas the sample which was kept darkened (squares) shows almost no decrease in intensity.

the previous experimental studies for single layer MoS_2 produced using mechanical exfoliation. Calculations of the band structures have suggested that for a single layer the band gap of MoS_2 is of the order of 1.97 eV, and furthermore, the transition is direct. That is, upon exfoliation to a single layer, MoS_2 is a direct band gap semiconducting material. This determination is supported by the observed photoluminescence, particularly as the energy of emission is also coincidental with the excitonic peak as shown in Figure 1. Typically, more than 65% of MoS_2 particles investigated showed this strong PL emission. Taken together with the observed thickness from AFM measurements and the frequency difference between peaks in the Raman spectra, a method for the production of highly concentrated suspensions of MoS_2 with a direct band gap in the visible-light region has been developed. There is also a small but broad peak observed at 1.99 eV which is likely due to emission from multiple particles as the incident laser spot is significantly larger than the lateral size of the exfoliated particles.

The photocatalytic properties of the single and few layer MoS_2 particles were investigated in the presence of visible light. To test the ability to catalyze redox reactions, the degradation of methylene blue was measured. Figure 6 shows the relative concentration of methylene blue (MB) as a function of exposure time to visible light (greater than 400 nm) in the presence of the suspended single and few layer MoS_2 particles. The concentration of particles used in this experiment was 20 ppm. As can be seen in Figure 6, the solution concentration of MB as determined from UV−vis spectrophotometry decreases rapidly with time. After 2 h, the concentration is less than 10% of the original solution indicating an efficient means for the photocatalytic degradation of a model dye system.

The results described above demonstrate that the surfactant-assisted sonication method for the production of single and few layer MoS_2 using continuous surfactant addition to increase the concentration of particles shows great potential for the large-scale production of this photocatalytic material. While a large proportion of particles are single layered and demonstrate strong photoluminescence, a distribution of sheet thickness is unavoidable using this technique. Judicious control over sedimentation can improve the relative proportion of single layer MoS_2; however, it is not possible to completely eliminate few layer particles.

In this study, the exfoliated MoS_2 particles have been sterically stabilized through the choice of polymeric block copolymer surfactants as the means for reducing surface tension. It is likely that the hydrophobic PPO block adsorbs to the particle surface with the hydrophilic PEO blocks extending out into solution. This steric stabilization mechanism is necessary as the liquid phase exfoliation produces particles with low surface charge which would otherwise rapidly flocculate due to strong interparticle dispersion forces. Previous studies have used monomeric ionic surfactants or oxidized the particles to increase surface charge and hence allow suspensions which are kinetically stable due to overlapping electrical double layers. To satisfactorily guard against rapid aggregation, substantially less than monolayer coverage (approximately 10%) of surfactant is required. Typically it is expected that the surfactant adsorbs to the basal planes and not edges as this results in more favorable hydrophobic−hydrophobic interactions. While the adsorbed surfactant necessarily reduces the available area for dye adsorption on the basal planes, it is expected that the catalytic sites are at the edge of the particles.

It should be apparent that though the block copolymers confer stability to the suspension the polymers would also be susceptible to photocatalytic degradation reactions similar to the model dye system studied herein. This should induce coagulation. On the time scale of the experiments presented in Figure 6, no such aggregation of the MoS_2 particles was observed; however, longer-term exposure to visible light may be required. Another advantage of this material is the vast available surface area allowing significant adsorption of the dye onto the particles even with the block copolymer present. As the reactions occur at the interface, the larger surface area to volume ratio gives rise to a highly efficient means for the degradation of the dye.

The stability of the MoS_2 particulate suspensions in water is obviously a key factor in the potential use in a range of photocatalytic applications including the splitting of water to form O_2 and H_2. MoS_2 has been suggested as a potential material for the photoelectrochemical production of hydrogen due to the magnitude of the band gap as well as the positioning of the bands relative to the potential.[30] Furthermore, the band gap is in the visible-light region, making it highly desirable for such an application due to the increased use of available solar

radiation in comparison to other materials such as TiO_2. Previous efforts have focused on 3D confinement effects for tailoring the band gap of MoS_2 first through the production of nanosized MoO_3 particles.[12,13] The sonication of MoS_2 in the presence of surfactant to produce single layer sheets is an alternate means for engineering the band gap, particularly as the transition has been shown to be direct upon exfoliation to a single sheet rather than indirect for the 3D nanoparticles. Thus, the strong photoluminescence of the particles produced in this manner also provides opportunities for use in sensing and coatings.

CONCLUSIONS

Concentrated suspensions of exfoliated MoS_2 nanoparticles were prepared through a sonication procedure with the interfacial energy of the solid and liquid phases matched by addition of surfactant continuously. Significantly higher concentrations of single and few layered MoS_2 were generated in comparison to batch procedures. Concentrations in excess of 100 ppm were easily achieved. The extinction coefficient for liquid phase exfoliated MoS_2 was measured from UV−visible spectrophotometry from known concentrations of particles determined from atomic absorption spectroscopy. Spectroscopic techniques showed that the exfoliated sheets were photoluminescent, indicating that a high proportion of the material was a single layer. The shift in E_{2g} and A_{1g} peaks in the Raman spectrum confirmed that the particles were exfoliated into molecularly thin sheets. These MoS_2 exfoliated sheets were used as a visible-light photocatalyst with the degradation of methylene blue demonstrated. The vast surface area afforded rapid adsorption of the material to the particle surface which greatly assists the redox reaction required to degrade the dye. Thus this procedure for preparing concentrated suspensions of semiconducting nanosheets of MoS_2 with bandgap of 1.97 eV shows great potential in photocatalytic applications.

AUTHOR INFORMATION

Corresponding Author

*E-mail: snotley@swin.edu.au. Tel.: +61 392148635.

Author Contributions

The manuscript was written through contributions of all authors. All authors have given approval to the final version of the manuscript.

Notes

The authors declare no competing financial interest.

ACKNOWLEDGMENTS

This project was supported through a grant from the Australian Research Council under the Future Fellowships scheme.

REFERENCES

(1) Geim, A. K. *Science* **2009**, *324*, 1530−1534.
(2) Geim, A. K.; Novoselov, K. S. *Nat. Mater.* **2007**, *6*, 183.
(3) Cheng, C.; Li, D. *Adv. Mater.* **2013**, *25*, 13−30.
(4) Sham, A. Y. W.; Notley, S. M. *Soft Matter* **2013**, *9*, 6645−6653.
(5) Allen, M. J.; Tung, V. C.; Kaner, R. B. *Chem. Rev.* **2010**, *110*, 132−145.
(6) Novoselov, K. S.; Jiang, D.; Schedin, F.; Booth, T. J.; Khotkevitch, V. V.; Morozov, S. V.; Geim, A. K. *Proc. Natl. Acad. Sci. U.S.A.* **2005**, *102*, 10451.
(7) Ramakrishna Matte, H. S. S.; Gomathi, A.; Manna, A. K.; Late, D. J.; Datta, R.; Pati, S. K.; Rao, C. N. R. *Angew. Chem., Int. Ed.* **2010**, *49*, 4059−4062.
(8) Coleman, J. N.; Lotya, M.; O'Neill, A.; Bergin, S. D.; King, P. J.; Khan, U.; Young, K.; Gaucher, A.; De, S.; Smith, R. J.; Shvets, I. V.; Arora, S. K.; Stanton, G.; Kim, H.-Y.; Lee, K.; Kim, G. T.; Duesberg, G. S.; Hallam, T.; Boland, J. J.; Wang, J. J.; Donegan, J. F.; Grunlan, J. C.; Moriarty, G.; Shmeliov, A.; Nicholls, R. J.; Perkins, J. M.; Grieveson, E. M.; Theuwissen, K.; McComb, D. W.; Nellist, P. D.; Nicolosi, V. *Science* **2011**, *331*, 568−571.
(9) Splendiani, A.; Sun, L.; Zhang, Y.; Li, T.; Kim, J.; Chim, C. Y.; Galli, G.; Wang, F. *Nano Lett.* **2010**, *10*, 1271−1275.
(10) Mak, K. F.; Lee, C.; Hone, J.; Shan, J.; Heinz, T. F. *Phys. Rev. Lett.* **2010**, *105*, 136805.
(11) Notley, S. M. *J. Colloid Interface Sci.* **2013**, *396*, 160−164.
(12) Thurston, T. R.; Wilcoxon, J. P. *J. Phys. Chem. B* **1999**, *103*, 11.
(13) Wilcoxon, J. P.; Newcomer, P. P.; Samara, G. A. *J. Appl. Phys.* **1997**, *81*, 7934−7944.
(14) Lotya, M.; Hernandez, Y.; King, P. J.; Smith, R. J.; Nicolosi, V.; Karlsson, L. S.; Blighe, F. M.; De, S.; Zhiming, W.; McGovern, I. T.; Duesberg, G. S.; Coleman, J. N. *J. Am. Chem. Soc.* **2009**, *131*, 3611−3620.
(15) Lotya, M.; King, P. J.; Khan, U.; De, S.; Coleman, J. N. *ACS Nano* **2010**, *4*, 3155−3162.
(16) Smith, R. J.; King, P. J.; Lotya, M.; Wirtz, C.; Khan, U.; De, S.; O'Neill, A.; Duesberg, G. S.; Grunlan, J. C.; Moriarty, G.; Chen, J.; Wang, J.; Minett, A. I.; Nicolosi, V.; Coleman, J. N. *Adv. Mater.* **2011**, *23*, 3944−3948.
(17) Blake, P.; Brimicombe, P. D.; Nair, R. R.; Booth, T. J.; Jiang, D.; Schedin, F.; Ponomarenko, L. A.; Morozov, S. V.; Gleeson, H. F.; Hill, E. W.; Geim, A. K.; Novoselov, K. S. *Nano Lett.* **2008**, *8*, 1704−1708.
(18) Hernandez, Y.; Nicolosi, V.; Lotya, M.; Blighe, F. M.; Sun, Z.; De, S.; McGovern, I. T.; Holland, B.; Byrne, M.; Gun'ko, Y. K.; Boland, J. J.; Niraj, P.; Duesberg, G.; Krishnamurthy, S.; Goodhue, R.; Hutchison, J.; Scardaci, V.; Ferrari, A. C.; Coleman, J. N. *Nat. Nanotechnol.* **2008**, *3*, 563.
(19) Hamilton, C. E.; Lomeda, J. R.; Sun, Z. Z.; Tour, J. M.; Barron, A. R. *Nano Lett.* **2009**, *9*, 3460−3462.
(20) Nuvoli, D.; Valentini, L.; Alzari, V.; Scognamillo, S.; Bon, S. B.; Piccinini, M.; Illescas, J.; Mariani, A. *J. Mater. Chem.* **2011**, *21*, 3428−3431.
(21) Wang, X.; Fulvio, P. F.; Baker, G. A.; Veith, G. M.; Unocic, R. R.; Mahurin, S. M.; Chi, M.; Dai, S. *Chem. Commun.* **2010**, *46*, 4487−4489.
(22) Chou, S. S.; Kaehr, B.; Kim, J.; Foley, B. M.; De, M.; Hopkins, P. E.; Huang, J.; Brinker, C. J.; Dravid, V. P. *Angew. Chem., Int. Ed.* **2013**, *52*, 4160−4164.
(23) Griffith, A.; Notley, S. M. *J. Colloid Interface Sci.* **2012**, *369*, 210−215.
(24) Notley, S. M. *J. Colloid Interface Sci.* **2012**, *375*, 35−40.
(25) Notley, S. M. *Langmuir* **2012**, *28*, 14110−14113.
(26) Zu, S. Z.; Han, B. H. *J. Phys. Chem. C* **2009**, *113*, 13651−13657.
(27) Guardia, L.; Fernández-Merino, M. J.; Paredes, J. I.; Solís-Fernández, P.; Villar-Rodil, S.; Martínez-Alonso, A.; Tascón, J. M. D. *Carbon* **2011**, *49*, 1653−1662.
(28) Lotya, M.; Rakovich, A.; Donegan, J. F.; Coleman, J. N. *Nanotechnology* **2013**, *24*, 265703.
(29) Molina-Sanchez, A.; Wirtz, L. *Phys. Rev. B* **2011**, *84*, 155413.
(30) Maeda, K. *J. Photochem. Photobiol. C* **2011**, *12*, 237−268.